Journal of Catalysis 273 (2010) 147–155

Contents lists available at ScienceDirect

Journal of Catalysis

journal homepage: www.elsevier.com/locate/jcat

Decoration of chitosan microspheres with inorganic oxide clusters: Rational design of hierarchically porous, stable and cooperative acid–base nanoreactors

Abdelkrim El Kadib [a,*], Karine Molvinger [b], Mosto Bousmina [a,c], Daniel Brunel [b,d]

[a] Institute of Nanomaterials and Nanotechnology (INANOTECH), ENSET, Av. De l'armée Royale, Madinate Al Irfance, 11100 Rabat, Morocco
[b] Matériaux Avancés pour la Catalyse et la Santé, Institut Charles Gerhardt, UMR 5253 CNRS/ENSCM/UM2/UM1, 8 rue de l'Ecole Normale, 34296 Montpellier Cedex 5, France
[c] Hassan II Academy of Science and Technology, Rabat, Morocco
[d] Instituto de Tecnología Química UPV-CSIC – Universidad Politécnica de Valencia, Av. de los Naranjos s/n – 46022 Valencia, Spain

ARTICLE INFO

Article history:
Received 8 April 2010
Revised 14 May 2010
Accepted 19 May 2010
Available online 22 June 2010

Keywords:
Chitosan microspheres
Supercritical drying
Bifunctional materials
Cooperative catalysis

ABSTRACT

One of the fundamental enzymatic catalyst assets, which is the most difficult to engineer in synthetic systems, is the coexistence of multifunctional sites and their synergetic cooperation. In this work, an efficient approach toward cooperative acid–base materials using natural matrices is proposed. Taking advantages from chitosan polysaccharide as nano-assembling system and on the supercritical drying technique to preserve their porosity, the mutual interactions between different glucosamine units and the Lewis acidic precursors (Ti, Zr, Al, Sn) allowed the preparation of hierarchically porous microspheres in which well-separated amino groups from chitosan are replicated with highly dispersed acidic inorganic oxides. This decoration at the nano-scale entails a notable improvement on the hydrothermal stability of the resulting organic–inorganic hybrid materials. The resulting acid–base hybrid materials are assessed for three carbon–carbon forming reactions (Henry condensation, Michael addition and jasminaldehyde synthesis) and systematically compared to the pure acidic inorganic oxide and basic chitosan microspheres. The bifunctional materials displayed interesting catalytic activity and selectivity, with respect to monofunctional ones, witnessing thus on the cooperative effect attainable in chitosan@inorganic oxide microspheres.

1. Introduction

The elucidation of the mechanisms by which many enzymes operate has revealed nature's use of multifunctional catalysis as a strategy for the optimization of chemical conversions [1–4]. Enzymes mutually immobilize incompatible functional groups in a manner that preserves untouched their respective functionalities, and therefore they are able to accelerate chemical reactions through synergic effect due to cooperative interactions between these precisely positioned reactive groups [5–7]. This paradigm of biological transformations has inspired the synthesis of a large library of homogeneous bifunctional acid–base catalysts, which exhibit superior activity and selectivity in many organic transformations, ranging from carbon–carbon bond-forming reactions to ring opening polymerization [8–14]. Moreover, the concept of frustrated Lewis acid–base pairs (FLP) demonstrated the power of these bifunctional species as organocatalyst [15,16]. The most spectacular finding was the ability of frustrated phosphinoborane to cleave hydrogen molecules, reactivity normally restricted to transition metal complexes, offering thus new opportunities for hydrogen storage, metal-free activation and catalysis. Generally speaking, acid–base bifunctional scaffolds display original properties that can be very efficient in coordination chemistry, material engineering and in catalysis.

Heterogeneous catalysis is undoubtedly more attractive than its homogeneous counterpart, because the use of solid catalysts guarantees cleaner, eco-friendly and economic processes and is clearly on the rise. Unfortunately, lower activity was commonly associated with this immobilization [17,18]. To circumvent this potential drawback, sustained efforts were directed to build an environment in which the active site and its support can collaborate [19–21]. In many examples, "metal–acid" or "metal–base" interactions turned out to be the key for better catalytic activity [22–29]. Surprisingly, materials operating by acid–base synergy and cooperative effects are relatively less addressed and stimulate a real challenge [30–35]. An early entry to investigate this concept was illustrated by the preparation of aluminophosphates and their use for fine chemical synthesis. The presence of weak acid–base pairs in these materials provides a potential activity and selectivity enhancement [36–38]. More recently, this idea re-emerged again in line with the interest for selective functionalization and engineering of the grafted active species in the mesoporous silica surfaces [39–44]. Ordered periodic mesoporous organosilicas hosting cooperative

* Corresponding author. Fax: +212 537570880.
E-mail addresses: a.elkadib@inanotech.ma, aelkadib@gmail.com (A.E. Kadib).

0021-9517/$ - see front matter © 2010 Elsevier Inc. All rights reserved.
doi:10.1016/j.jcat.2010.05.010

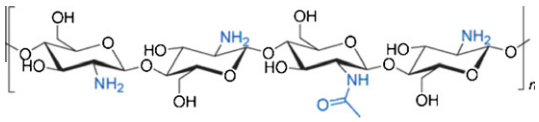

Scheme 1. Structure of chitosan.

positioned sites in their framework are reported [45–50]. However, the multifunctionalization of mesoporous silica supports with a control of the relative concentration and proper spatial arrangement of the different functional groups is not easy to tune, time-consuming and energy demanding, which can overwhelm the benefit of the catalysts and their suitable scalability.

In our course to design materials from renewable resources [51–53], we recently initiated a research program aimed to explore the potential use of polysaccharide macromolecules as hierarchical supports for catalysis [54–58]. Designing catalysts that satisfy all the criteria of heterogeneous solids from naturally available materials constitutes a valuable alternative to synthetic mesoporous materials. In this context, one of the more attractive polysaccharide polymers is chitosan (obtained from chitin): the second most abundant organic resources next to cellulose, with a production estimated to be several billion tons per year [59]. Beside their biocompatibility and biodegradability, chitosan macromolecules feature well-dispersed amino groups (~5.8 mmol), which confers them a basic character for use in catalysis or as Schiff base to coordinate transition metals (Scheme 1) [53–67].

Moreover, the secondary structure of a chitosan gelling polymer is able to assemble at the nano-scale offering thus the possibility to design materials with hierarchical porosity, controlled size and sophisticated arrangements of functional groups, with well dispersion over its precise geometry [68–71]. Hitherto, the use of polysaccharide polymers in catalysis was limited by their poor stability and lower porosity [72,73]. However, their silica mineralization by sol–gel process resulted in more robust organic–inorganic siliceous materials featuring highly dispersed amino groups in the matrices [55,65]. In addition, the CO_2 supercritical drying ($scCO_2$) of these microspheres was found to be extremely efficient to obtain high surface area hybrid materials [54–57].

Expending the scope of this mineralization to more reactive inorganic oxides and looking for successful acid–base cooperation are the two goals addressed in this contribution. Herein, we describe an unprecedented rational design of bifunctional acid–base catalysts generated by replication of chitosan microspheres by inorganic oxide clusters (titania, zirconia, alumina and tin oxide) by sol–gel mineralization process. Their textural properties are highly improved by CO_2 supercritical drying technique. Their catalytic behavior in three organic transformations (Henry condensation, Michael addition and jasminaldehyde synthesis) shed more light on their acid–base cooperation and synergy. This strategy bears opportunities that will further advance the potential application of polysaccharide-based materials in catalysis.

2. Experimental

2.1. Chemicals

Chitosan (Aldrich high molecular weight, 20% acetylation) was used as the polymeric component. $Ti(acac)_2(iOPr)_2$, $Ti(iOPr)_4$, $Ti(OBu)_4$, $Zr(OBu)_4$, $Al(OEt)_3$, Sn(hexadecanoate)$_2$ are purchased from Aldrich and used as received. Nitromethane, cyanoethylacetate and heptanal are used without further purification. Prior to use, benzaldehyde and methyl vinyl ketone are distilled and stored under inert atmosphere (argon).

2.2. Characterization of materials

Nitrogen sorption isotherms at 77 K were obtained with a Micromeritics ASAP 2010 Micromeritics apparatus. Prior to measurement, the samples were degassed for 8 h at 80 °C for hybrid inorganic oxide@chitosan microspheres and at 250 °C for pure inorganic oxides. The surface area (S_{BET}) and the C_{BET} parameter were determined from BET treatment in the range 0.04–0.3 p/p_0 and assuming a surface coverage of nitrogen molecule estimated to 13.5 Å^2. The mesoporous volume and the pore diameter were evaluated from the adsorbed gas amount when the capillary condensation is ended and from the BJH model, respectively. Thermogravimetric analyses were performed with a Netzsch TG 209 C apparatus. XRD were performed on D8 Advance Bruker AXS (powder diffraction, geometry: Bragg Brentano). Supercritical CO_2 drying was performed by using a Polaron 3100 apparatus (74 bar, 31.5 °C). SEM images were obtained using a Hitachi S4500 microscope, and EDX measurements were carried out using FEI 200F quanta 200F connected to the SEM Hitachi S4500 microscope. TEM images were obtained using JEOL 1200 EX II (120 kV). DRIFT spectra were performed on Bruker vector 22. XPS analyses were performed at room temperature with an SSI 301 spectrometer using monochromatic and focused (spot diameter) 600 μm, 100 W) Al K R radiations (1486.6 eV) under a residual pressure of 10^{-7} Pa. Charge effects were compensated by the use of a flood gun (5 eV). The hemispherical analyzer functioned at constant pass energy of 50 eV. The experimental bands were fitted to theoretical bands (80% Gaussian, 20% Lorentzian) with a least squares algorithm using a nonlinear baseline. Reference binding energy was C1s of CH_3 and of the contamination carbon at 284.6 eV. DRX were performed on D8 Advance Bruker AXS (powder diffraction, geometry: Bragg–Brentano). UV–visible (DRUV) spectra were measured in the 200–800 nm range using $BaSO_4$ as the reference on a Perkin-Elmer Lambda 14 spectrometer equipped with an integrating sphere (Labsphere, North Sutton, USA). Quartz cells (Hellma) of 0.05 mm path length were used. 13C MAS NMR spectra were acquired on a Bruker Avance 300 DPX spectrometer operating at 75.467 MHz under cross-polarization conditions.

2.3. Synthesis of hybrid microspheres

2.3.1. Synthesis of chitosan microspheres *M0*

The synthesis of porous chitosan microspheres as precursors was carried out according to Ref. [54]. An aqueous solution of chitosan was obtained by dissolving 1 g of chitosan in 100 mL of a solution of acetic acid (0.055 mol L^{-1}) corresponding to a stoichiometric amount of acid with respect to the amount of NH_2 functions. Total dissolution was obtained under stirring over one night at room temperature. This solution was dropped into a NaOH solution (4 N) through a 0.8-mm gauge syringe needle providing gelified chitosan microspheres. The chitosan beads were stored in the alkaline solution for 2 h and then washed copiously with distilled water until neutral pH to lead hydrogel microspheres. Then, hydrogel was dehydrated by immersion successively in a series of ethanol–water baths containing more and more ethanol from pure water to 100% ethanol to provide alcogel microspheres. Ethanol is exchanged again with CO_2 and then the microspheres are dried under supercritical conditions. The resulting aerogel material was denoted **M0**.

2.3.2. Synthesis of chitosan@inorganic oxide hybrid aerogel microspheres

The metallic solution was prepared with an appropriate polymerizable precursor (see Table 1) which is dissolved in isopropanol (Precursor: iPrOH = 1:10) (similar results are obtained when ethanol used as solvent). The beads of chitosan (250 mg) were dipped

Table 1
Textural properties of microspheres.

Entries	Materials	Precursor	% Mineral[a]	S_{BET}[b] (m^2/g)	V[b] (cm^3/g)	Pore diameter[b] (Å)	C_{BET}[b]
1	**M0**	–	0	120	0.34	85	142
2	**M1H**[c]	$Ti(acac)_2(OiPr)_2$	25	480	1.86	112	70
3	**M2H**[c]	$Ti(OiPr)_4$	29	450	1.29	71	58
4	**M3H**	$Ti(OtBu)_4$	25	370	0.94	110	63
5	**M4H**	$Zr(OtBu)_4$	32	236	0.60	98	67
6	**M5H**	$Al(OEt)_3$	27	288	1.11	115	52
7	**M6H**	$Sn(acac)_2$	42	243	0.55	71	64
8	**M7H**	$Zr(acac)_2$	9	201	1.39	89	95
9	**M8H**	$Al(OiPr)_3$	4	216	1.57	101	88
10	**M9H**[d]	$Si(OEt)_4$	67	157	0.33	129	111

[a] Determined by TGA.
[b] From nitrogen sorption analysis.
[c] Data from Ref. [56].
[d] The casting of silica was performed under acidic conditions (HCl/H_2O) as described in Ref. [55].

in the metallic solution (4 mmol) at room temperature for 48 h. The microspheres were washed first with isopropanol twice and then with ethanol. Ethanol was again exchanged with CO_2. Hybrid microspheres were dried by supercritical CO_2 to afford aerogel porous hybrid microspheres **M1H–M6H**. The preparation of **M1H** and **M2H** was already described in Ref. [56].

2.3.3. Preparation of pure inorganic oxide microspheres

The hybrid chitosan@inorganic oxide aerogels **M1H–M6H** are calcined for 6 h at 550 °C under air (rate: 20 °C/min) to give pure titania, zirconia, alumina and tin oxide, which we used only for comparison in catalysis.

2.3.3.1. Catalysis. For the three reactions, catalysis was carried out under argon. Before catalysis, beads were introduced in a flask and activated by heating in batch oil at 50 °C under vacuum for 1 h and then the flask was purged with nitrogen and kept in an inert atmosphere. Solvent and reactants are added at room temperature, and the zero time of reaction was taken when the temperature reached, respectively, 80 °C for Henry reaction and 80 or 120 °C for jasminaldehyde synthesis. Reaction progress was monitored via examination of aliquots obtained from the reaction mixture by GC (FID), using dodecane as an internal standard and a calibration curve to quantify the FID response. The heterogeneous catalyst was recovered by sample removal of the beads and washing the collected solids with copious amounts of ethanol following their CO_2 supercritical drying.

In a typical procedure for Henry reaction, 0.05 mmol of the catalyst is activated for 1 h at 50 °C. Then, 1 mmol of 4-methoxybenzaldehyde and 8 mL of nitromethane are introduced. The temperature is increased to 80 °C, and the reaction progress was monitored by GC analysis. In Michael addition, ethyl cyanoacetate (1 mmol) and methylvinylketone (2.2 mmol) are introduced in a flask containing 0.05 mmol of activated catalyst. For jasminaldehyde synthesis, 0.05 mmol of activated catalyst was immersed in 10 mL of distilled toluene. Then, benzaldehyde (5 mmol) and heptanal (1 mmol) are introduced.

3. Results and discussions

3.1. Preparation of the materials

The preparation of the bifunctional chitosan@inorganic oxide hybrid materials is a multistep process starting from chitosan alcogel microspheres. First, dropping an acetic acid chitosan solution into the NaOH coagulation bath forms stable hydrogel microspheres [54]. Chitosan alcogel beads are then obtained after exchange of water by ethanol through successive immersions in a series of ethanol–water baths by increasing the ethanol solution. This swelled polymer is characterized by very open structure, with a macroporous void volume of ~96%, and can be easily impregnated by an isopropanol solution of processable sol–gel metallic precursors (Table 1). Protracted stirring in these solutions allows the diffusion of the inorganic species inside the polymer. Thanks to the weak interaction $NH_2 \rightarrow M$ (M = Ti, Zr, Al, Sn), the metallic precursors were efficiently scavenged by polysaccharide matrices and the inorganic species were grown between the fibrils of chitosan by the so-called "coordination expansions" [74]. By optimizing the reaction conditions, this strategy universally allowed the entanglement of 25–42% of metallic oxides clusters (entries 2–7, Table 1). The kinetic of hydrolysis and condensation of the starting precursors has no significant effect on the homogeneity and inorganic oxide loading since the three titanium precursors led to similar results (entries 2–4, Table 1). However, the solubility seems to be determinant for this nanocasting strategy. This was illustrated in the preparation of chitosan@zirconia hybrids for which two different precursors were used: $Zr(acac)_2$ and $Zr(OtBu)_4$. The higher percentage of ZrO_2 in **M4H** (32%) compared to **M7H** (9%) can be explained by the higher solubility of $Zr(OtBu)_4$ than $Zr(acac)_2$. This ensures a better homogeneity of the solution, an excellent contact between the zirconia sol-solution and the chitosan microspheres. Under these conditions, the diffusion is better and the inorganic oxide part increases. Similar tendency is observed for aluminum incorporation: $Al(OEt)_3$ is more soluble than $Al(OiPr)_3$, so the percent of alumina nanoclusters is greater in **M5H** than in **M8H**.

3.2. Morphology and textural properties of the hybrids

To keep the porous texture of these hybrid alcogels, the microspheres were dried under CO_2 supercritical conditions. This drying method was first reported by Kistler 78 years ago for the preparation of expanded aerogels including mineral oxides, gelatine, agarose and other organic polymers [75]. This methodology has been further investigated to stabilize the texture of silica gels [76–79], titania-silica mixed oxides [80] and alumina aerogel [81–83]. In this kind of treatment, water or isopropanol is replaced by a solvent (CO_2), which is itself extracted beyond its critical point. In this way, the supercritical extraction of the pore fluid from a wet gel prevents the network collapse that is otherwise induced by capillary forces. These ones developed during the drying process of gels are given by the relation (1) [84]:

$$Pc = 2\sigma\cos(\theta_c)/r_p \quad (1)$$

where Pc is the capillary pressure, σ is the interfacial liquid/vapor surface tension, r_p is the capillary radius and θ_c is the solid/liquid contact angle. Hence, supercritical drying was used to eliminate

the capillary pressure through elimination of σ and the aerogel formed is expected to reproduce in the dry state the texture of the original gel.

Nitrogen sorption analysis confirmed the porous character of the network of the hybrid microspheres after $scCO_2$ drying (Table 1). The surface areas are found to range from 236 m^2/g to 480 m^2/g (entries 2–7, Table 1). The isotherm profile suggests a dual meso-macroporous network featuring pore sizes larger than 50 nm (Fig. S1). Native chitosan **M0** obtained by CO_2 supercritical drying of the beads displays a similar porous network, with a surface area of 120 m^2/g (entry 1, Table 1). Notably, the materials resulting from the diffusion of inorganic alkoxides in the matrix and their subsequent mineralization show an additional porosity. This suggests that inorganic alkoxides behave as a swelling agent for organic polymer. The M–O–M condensation occurring inside the chitosan alcogel induces a sort of coating of chitosan fibers. This decoration with metal oxide decreases the textural shrinkage occurring during the change from alcogel to aerogel, although the $scCO_2$ drying lowers this phenomenon compared to the other types of polysaccharide drying [54]. Nitrogen sorption analysis ruled out the presence of microporous networks that can be created by a nontemplated polymerization of inorganic alkoxides. This highlights the efficiency of chitosan to direct the sol–gel mineralization of these inorganic precursors. SEM analysis of all hybrid materials shows a fibrillar network characteristic of chitosan polymer (Fig. 1). The fibers are well isolated and no collapse of the network was observed, witnessing the efficacy of the supercritical drying to improve their textural properties. TEM analyses were performed to get more insight into the dispersion of inorganic oxides inside the hollow microspheres. For all the materials investigated, the mineralized inorganic oxides seem to grow following a fibrous axis, which suggested a strong interplay with chitosan fibers. In addition, the growth seems to occur homogeneously and no bulk materials or separated phases were found (Fig. S2).

In mapping the location of inorganic species across the microsphere, their radial distribution was determined by energy dispersive X-ray (EDX). The results indicate that the metal clusters are homogenously dispersed but their concentration increases slightly toward the outer shell (Fig. S3). However, the materials do not display a pure core–shell structure as found for chitosan@SiO_2 hybrid [55]. The absence of any peaks in X-ray diffraction analysis indicates that these nanosized inorganic species are amorphous and no crystalline particles exist in the materials.

3.3. Chemical structure of the hybrid microspheres

To establish the chemical structure of these hybrid materials, NMR, DRIFT, DRUV and XPS analyses were performed. MAS ^{13}C NMR of all hybrid microspheres was performed and compared with the literature data of polymeric chitosan [64]. All spectra exhibited two peaks around 24–26 and 174 ppm, which can be assigned to methyl and carbonyl groups, respectively. Peaks at 55, 75, 82 and 105 ppm can be assigned to $C_{2,6}$, $C_{3,5}$, C_4 and C_1, respectively (Fig. S4). This indicates that no transformation occurred on the polymeric chain during the formation of these nanocomposite materials. DRIFT analysis revealed essentially the characteristic bands of polymeric chitosan. Indeed, a broad and unstructured absorption at 3700–3000 cm^{-1} due to the overlap of OH and NH stretching vibration bands is observed. Characteristic bands of CH_2 and CH_3 are also observed at 2950 cm^{-1}. Deformation of NH_2 and NH are also shown around 1600 cm^{-1}. DRUV analysis shows, in the particular case of chitosan@titania hybrids, a broad oxygen → metal charge-transfer (CT) adsorption bands with maxima at 312 nm (**M1H**); 280 nm (**M2H**) and 285 nm (**M3H**) (Fig. S5). This adsorption is consistent with an incipient oligomerization of Ti(IV) species [85–87].

XPS analysis of the ground samples provided additional information about the distribution of metallic oxide species across the microspheres (Table S1). First, it was found that the percent of inorganic oxide clusters was slightly more important (by ~4%) at the surface than in the bulk, in agreement with EDX distribution analysis. The presence of absorption peaks at 458.3 eV, 458.5 eV and 458.4 eV for **M1H, M2H** and **M3H**, respectively, confirms the presence of titanium oligomeric clusters inside the beads matrices [88]. The presence of zirconia, alumina and tin oxide was corroborated by the presence of peaks at 182.9 and 181.8 eV for **M4H**, 74 and 74.2 eV for **M5H**, 182.9 and 181.8 eV for **M4H** and at 486.5 and 486.3 eV for **M6H**, respectively. The presence of two peaks around 399 eV and 400 eV indicates the presence of two nitrogen species. The former at 399 eV is characteristic of free amine (NH_2); the second at 400 eV can be attributed to the protonated NH_3^+ or lower metal coordinated NH_2 → M.

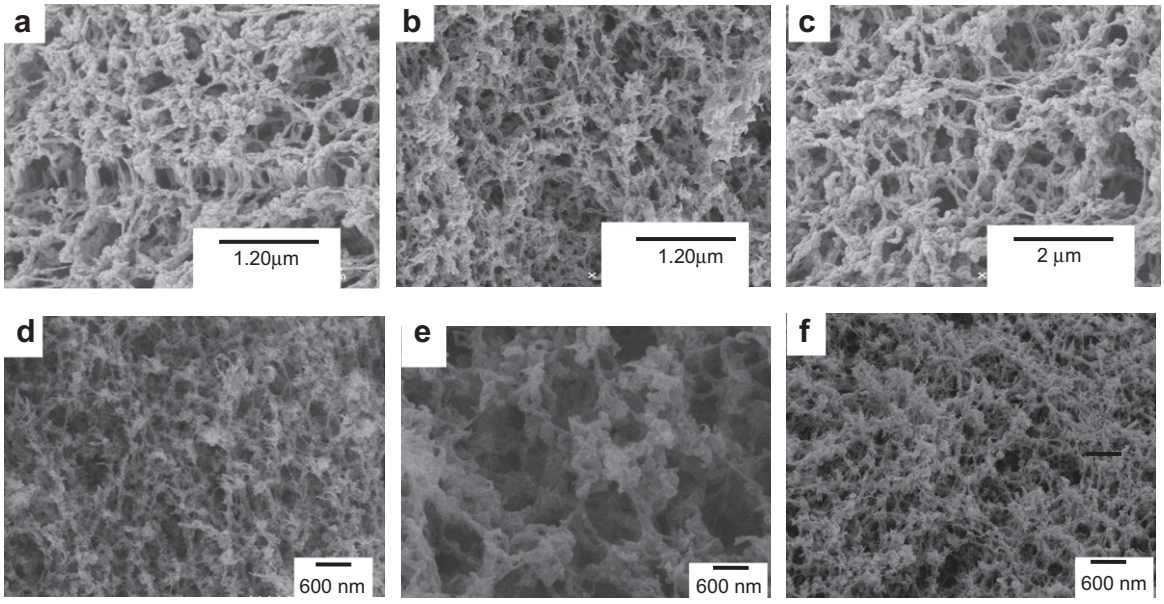

Fig. 1. SEM analysis of: (a) **M1H**, (b) **M2H**, (c) **M3H**, (d) **M4H**, (e) **M5H** and (f) **M6H**.

3.4. Stability and surface state of the hybrid microspheres

The chemical stability and mechanical robustness of these materials are the key factors for their use in catalysis. We previously evidenced that chitosan@TiO_2 displayed a better chemical and hydrothermal stability than the native chitosan and chitosan@SiO_2 [56]. Hence, we were interested to further assess the hydrothermal stability of chitosan@Al_2O_3, chitosan@ZrO_2 and chitosan@SnO_2. The stability tests consisted in the treatment of the beads in aqueous solution under reflux (~100 °C) for 2 h, and the network texture was then investigated by SEM and nitrogen sorption analyses (Fig. S7 and Table S2). As expected, the mineralization of chitosan by these inorganic species resulted in an improvement on their stability as evidenced by the preservation of the porosity and the fibrillar network. By contrast, refluxing chitosan **M0** and chitosan@SiO_2 resulted in a complete collapse of the matrices. The former result was expected since organic polymers generally suffer from lower thermal and hydrothermal stability. The mineralization by silica is not really a judicious choice as the continuous degradation of mesoporous silica under hydrothermal and basic conditions constituted a deterrent to their use as catalyst in aqueous or basic media [84,89–91]. Moreover, the grafted amine moiety reacts with the functionalities of silica support in different ways causing the collapse of the network and reducing thus the life time of these catalyst supports and their stability [84,92–94]. From all these results, two striking points came out: first (i) the basicity of chitosan and the acidity of inorganic oxides are compatible and turned out to guarantee the adhesion of the two partners. Second, (ii) these inorganic species act as a protective layer and prevent the damage of organic fibrils. This suggests a pronounced hydrophobic character of these materials when compared to the native chitosan microspheres **M0**.

These assumptions are somehow confirmed by nitrogen sorption analysis. The use of the Brunauer Emmett Teller (BET) model allows deriving a parameter (C_{BET}) indicator of this property. It is defined as $C_{BET} \approx \exp(E_1 - E_L)/RT$, which relates the interaction strength of the first adsorbed monolayer when compared to the interaction of any other adsorbed layer with the surface, taken as the liquefaction enthalpy [95–97]. The comparison of the values summarized in Table 1 shows that native chitosan possess the highest C_{BET} parameter among the series of the materials (entry 1, Table 1). After mineralization, a dramatic decrease in the C_{BET} values was observed passing from 120 to 60–65. This is consistent with the replication of inorganic oxides around polysaccharide fibrils, which occurs by consumption of various hydroxyl and amino groups that lead to more hydrophobic C–O–M and M–O–M on the surface. During calcination, the cleavage of C–O–M bonds attaching the organic and inorganic parts occurs, and more polar and reactive hydroxyl groups M–OH are generated on the surface of the material; consequently, C_{BET} increases again (Fig. 2).

3.5. Catalytic results

Stimulated by the presence of both basic primary amino groups (NH_2) from chitosan polymer and the acidic nanosized inorganic oxide clusters, we anticipated that this coexistence might lead to synergic and cooperative effect in catalysis. In addition, the comparison will allow selecting the more efficient pair "chitosan@inorganic oxide" combination in catalysis and drawing, whenever possible, some conclusions concerning the influence of the Lewis acidity of the metal on the catalytic activity [98].

We selected three organic transformations (Henry reaction, Michael addition and jasminaldehyde synthesis) which are considered as sensible to the acid/base synergy. Significant improvement in the catalytic activity was observed when Henry reaction of nitromethane with 4-methoxybenzaldehyde was subjected to

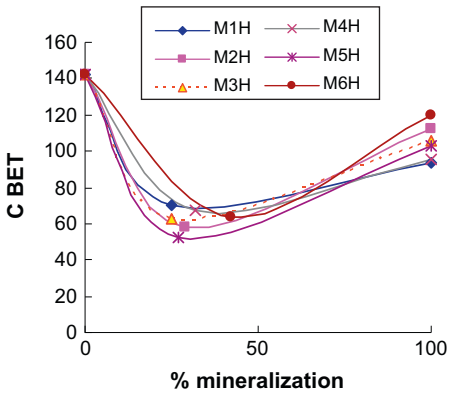

Fig. 2. C_{BET} variation as a probe of hydrophilic–hydrophobic switch during mineralization.

acid–base homogeneous [99–102] and heterogeneous catalysts [35,39,47–49]. We then focused on the assessment of the catalytic activity of chitosan@inorganic oxide microspheres for this reaction. The catalytic performances using these catalysts among different materials are shown in Table 2. One of the more important result of the present study is the higher reactivity of the bifunctional catalysts (entries 4–9) compared to the monofunctional chitosan **M0** (entry 3) or pure inorganic oxides (entries 10–13). The reaction proceeds smoothly with chitosan, and a quantitative yield is achieved after 24 h of reaction (entries 2 and 3). At the same time, all tested inorganic oxides revealed poor reactivity (entries 10–13). This demonstrates that the basicity plays a crucial role for accelerating the reaction and no discrimination was observed among all these hybrids in terms of the activity even though chitosan@Al_2O_3 was slightly less active (entries 10–13). Moreover, no discrepancy in the selectivity was observed indicating that basically they are all operating in the same manner. The predominance of nitrostyrene **1** versus nitroalcohol **2** suggests that the condensation occurs by an imine formation mechanism. This is consistent with the reactivity of primary amine supported silica that produced preferentially nitrostyrene [103]. In contrast, tertiary amine switched the selectivity to nitroalcohol as a consequence of an ion pair mechanism [103]. There are many precedents in the literature claiming cooperative effect between primary amine and surface silica supports [39,49,104,105] and between primary amine and sulfonic, phosphoric and carboxylic acids [106]. Surface acidic silanols (Si–OH) accelerate imine and iminium formation, both of which are intermediates in nitrostyrene formation. Similarly, the systematic higher reactivity of the hybrids compared to the native chitosan can be mainly explained by an assistance of metallic Lewis acid during the imine formation (Scheme 2).

We further investigate catalysis of Henry reaction by homogenous base, inorganic alkoxide precursors and their association. As expected, the activity of the bases follows their strength and the selectivity depends on the amine nature (primary versus tertiary amine) (entries 14–16, Table 1). Again, moderate activity was found for all inorganic alkoxides (entries 17–20, Table 1). More importantly, the efficiency of triethylamine or ethylamine was inhibited in the presence of a stoichiometric amount of metallic alkoxide (entries 21 and 22). It has been reported that propylamine and aminopropyltriethoxysilane coordinate titanium alkoxide precursors leading to transient OiPr bridged dimeric form [74], which are chemically inactive because of the neutralization effect between the Lewis base and Lewis acid. The simultaneous introduction of chitosan **M0** and calcined inorganic oxides, inspired by the concept of site isolation [30–33], does not lead to any further improvement. We previously demonstrated that inorganic oxide solids cannot diffuse inside the chitosan matrices, thus excluding

Table 2
Henry reaction of nitromethane with 4-methoxybenzaldehyde.[a]

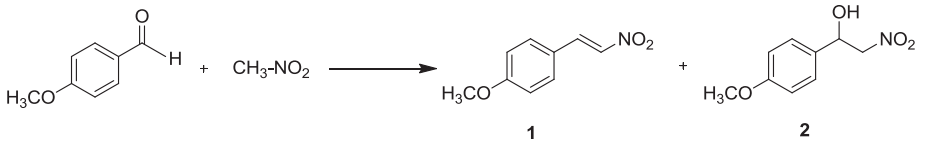

Entry	Cat.	*t* (h)	% Convn.	**1** (%)	**2** (%)
1	–	24	0	–	–
2	**M0**	3	15	95	5
3	**M0**	24	68	95	5
4	**M1H**[b]	3	98	97	3
5	**M2H**[b]	3	90	93	7
6	**M3H**[b]	3	95	95	5
7	**M4H**	3	82	96	4
8	**M5H**	3	76	91	9
9	**M6H**	3	93	97	3
10	TiO_2	24	7	100	0
11	ZrO_2	24	14	63	27
12	Al_2O_3	24	10	84	16
13	SnO_2	24	26	92	8
14	NEt_3	5	55	29	71
15	Et-NH_2	5	90	92	8
16	Ph-NH_2	24	13	81	19
17	$Ti(OiPr)_4$	24	16	94	6
18	$Zr(OBu)_4$	24	13	81	19
19	$Al(OEt)_3$	24	15	93	7
20	$Sn(Acac)_2$	24	26	96	4
21	$Et_3N/Ti(OiPr)_4$	24	0	–	–
22	Et-NH_2/$Ti(OiPr)_4$	24	0	–	–

[a] See experimental section for details.
[b] From Ref. [57].

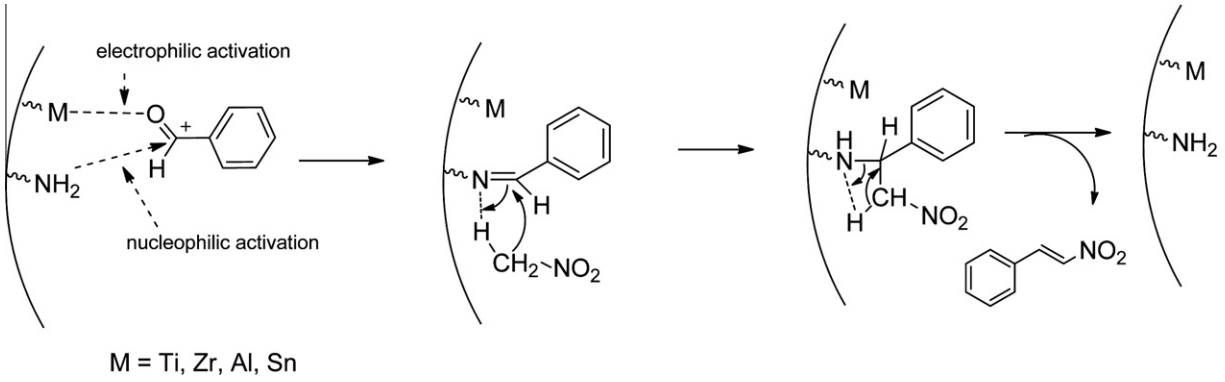

Scheme 2. Suggested imine catalytic mechanism for the production of nitrostyrene.

the possibility of acid–base pair's neutralization. This highlights that the two involved basic and acidic sites have to be in close proximity to collaborate.

These preliminary results encouraged us to investigate other reactions for which the synergy can be beneficial in terms of both the activity and the selectivity. Michael addition, involving electrophilic activation, constitutes a valuable strategy to construct complex building blocks by carbon–carbon forming reaction. Hence, investigation into the addition of 2 equiv. of methyl vinyl ketone to the activated ethyl cyanoacetate allows drawing some concluding remarks about the behavior of these catalysts (Table 3). In terms of conversion, all hybrid materials allowed a quantitative conversion in 30 min (entries 2–7, Table 3), whereas with native chitosan **M0**, a moderate yield was reached after an extended time of 1 h (entry 1, Table 3). This evidences the advantages of the hybrids over native chitosan microspheres. It is notable that no further improvement was observed by the introduction of both chitosan and inorganic oxide beads. Regarding the selectivity, all the hybrid materials gave a good selectivity for 5-carboethoxy-5-cyano-2,8-nonandione **4**. In the case of chitosan **M0**, however, the conversion did not exceed 58%. Since the proton of **3** is less acidic than that of the ethyl cyanoacetate, the carbon–carbon bond-forming reaction cannot occur only through the single activation of nucleophile by amine functions especially under our mild conditions. This demonstrates the beneficial effect of the electrophilic activation of the carbonyl group acceptor by metallic oxide nanoparticles. Similarly, a significant enhancement of catalytic activity gained by supporting organic amines in silica–alumina (Si–O–Al) was recently reported [47]. This unusual activity was also rationalized by the dual acid–base character of the designed materials, which makes them more reactive than the classical amine supported silica catalysts [47].

Table 3
Michael addition of ethyl cyanoacetate with 2 equiv. of methyl vinyl ketone.[a]

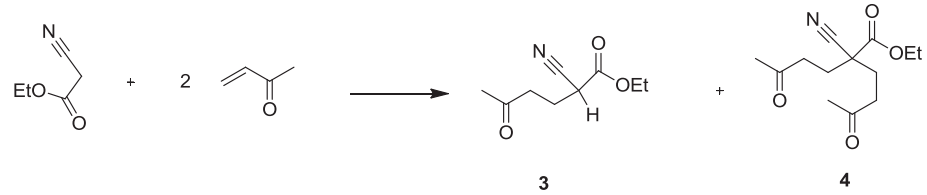

3 **4**

Entry	Cat.	*t* (h)	% Convn.	**3** (%)	**4** (%)
1	**M0**	1	41	43	57
2	**M1H**[b]	0.5	78	3	97
3	**M2H**[b]	0.5	70	21	79
4	**M3H**[b]	0.5	70	13	87
5	**M4H**	0.5	62	8	92
6	**M5H**	0.5	70	13	87
7	**M6H**	0.5	90	0	100
8	TiO_2	3	35	64	36
9	ZrO_2	3	22	54	36
10	Al_2O_3	3	16	38	62
11	SnO_2	3	41	19	81

[a] See experimental section for details.
[b] From Ref. [57].

The last catalytic application concerns the synthesis of jasminaldehyde(-2-pentyl-3-phenyl-2-propenal **5**, an important perfumery chemical, which is prepared industrially through the condensation of 1-heptanal and benzaldehyde in the presence of alkali as a catalyst (sodium or potassium hydroxide). However, the serious drawback of this route concerns the formation of an undesirable 2-pentyl-2-nonenal **6** from the self-condensation of heptanal. Attempts to resolve this problem can be broadly divided into the use of solid materials with shape selectivity [36] or bifunctional acid–base catalysts. In the latter case, a series of catalysts were investigated including HY and β-zeolites [36], aluminosilicates [107], magnesium organosilicates [108], amorphous aluminophosphates [36,38], 2D hybrid germanium zeotype [109] and so on. From a mechanistic viewpoint, the weak acidic site induces an electrophilic activation of the carbonyl group of benzaldehyde, which favors the attack of the enolate heptanal intermediate formed by interaction with the basic sites. Based on this rational, the catalytic activity of these hybrid microspheres was explored and the obtained results are summarized in Table 4. The hybrids perform a quantitative conversion of heptanal in a relatively short reaction time compared with the monofunctional chitosan **M0** or inorganic oxide for which the reaction needs more time to reach nearly the same conversion. To our delight, the results obtained with the bifunctional hybrid materials are encouraging particularly in terms of the selectivity (entries 2–7, Table 4). Up to 69% of the targeted jasminaldehyde product was obtained with all these chitosan@inorganic oxides with a remarkable selectivity of 86% obtained with **M1H** (entry 2, Table 1). This value is very close to that achieved by bifunctional aluminophosphate $AlPO_4$ [36,38], the best selective catalyst, to our knowledge, for jasminaldehyde synthesis.

3.6. Recycling and heterogeneous nature of the reaction

Beside the catalytic activity of the conceived materials, there are other parameters to take into consideration specifically in heterogeneous systems. There have been numerous cases in which the

Table 4
(*E*/*Z*)-2-pentyl-3-phenyl-2-propenal synthesis.[a]

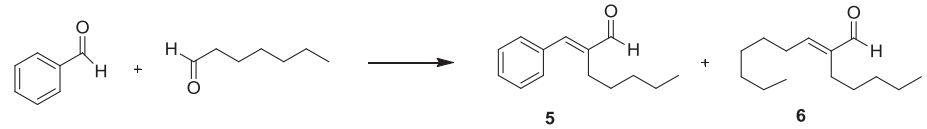

5 **6**

Entry	Cat.	*t* (h)	Temp. (°C)	Convn. heptanal (%)	**5** (%)	**6** (%)
1	**M0**	6	80	92	48	50
2	**M1H**[b]	4	80	98	86	11
3	**M2H**[b]	4	80	85	81	9
4	**M3H**[b]	4	80	89	79	12
5	**M4H**	4	80	76	71	25
6	**M5H**	4	80	81	69	23
7	**M6H**	4	80	92	81	6
8	TiO_2	24	120	87	53	19
9	ZrO_2	24	120	66	31	65
10	Al_2O_3	24	120	51	16	75
11	SnO_2	24	120	92	61	23

[a] See experimental section for details.
[b] From Ref. [57].

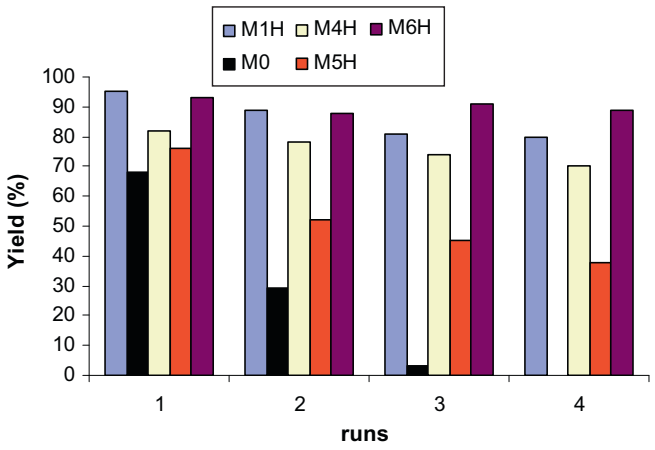

Fig. 3. Reusability of the microspheres in Henry condensation.

use of supposedly heterogeneous catalysts has resulted in leaching of the active site at levels which made the true heterogeneity of the catalysis to be questionable. To rule out the possible role played by chitosan microspheres as a reservoir to catch and release highly active metallic nanoparticles during catalysis, leaching experiments were systematically performed for Henry reaction. This consists in hot filtration during the course of reaction (at ~50% conversion), while the reaction mixture still hot to prevent any metal redeposition. Upon removal of the beads, no further conversion was observed even after a prolonged time (Fig. S7). In addition, no metallic species were observed by analyzing the filtrate by ICMPS. These findings are to some extent suggestive of the heterogeneous nature of these reactions.

Recyclability is obviously a critical feature of supported catalysts. Interestingly, these hybrid materials displayed good reusability both for Henry condensation (Fig. 3) and for Michael addition (Fig. S8). **M1H**, **M4H** and **M6H** maintain their catalytic activity although a prolonged reaction time was necessary to achieve complete conversion. By contrast, chitosan@Al_2O_3 **M5H** was found to be less reusable and a significant loss of activity was observed. Despite this fact, it is clear that the mineralization of chitosan brings additional advantages to their use in catalysis. This was evidenced by studying the reusability of native chitosan **M0** (Fig. 3). It was found that a faster deactivation took place with only 3% of conversion in the third run, whereas the hybrids were found to be more reusable with chitosan@TiO_2 and chitosan@SnO_2 performing up to 80% during the fourth run.

The reused materials were subjected to nitrogen sorption and SEM analysis in order to evaluate the evolution of the network (Fig. S9). Consistent with their higher stability, the recycled hybrids were still porous and no collapse of the fibrils was observed, despite a slight decrease in their surface area. This reusability is remarkable since many solid materials (especially organic polymers) showed a faster decay because of their textural alteration and/or chemical poisoning.

4. Conclusion

In summary, a straightforward strategy for designing bifunctional hybrid chitosan@inorganic oxide was reported in this work. The particular self-assembly properties of chitosan in addition to the mutual chemical interactions between the glucosamine units and the Lewis acid precursors were found to control the condensation of inorganic oxide inside the beads of chitosan. The intimate mixing of organic and inorganic frameworks entails a notable improvement on the textural properties and the hydrothermal stability of the resulting materials when compared to the individual component ones.

The cooperative effect in catalysis is not really a new phenomenon since many authors reported on it several years ago. It is notable, however, that the catalysts described in this work provide the first example of bifunctional acid–base materials built from renewable resources. Three main features of these new hybrid microspheres appear to be very relevant for catalytic application: (i) the higher surface areas and the macroporous network of these microspheres which are important for the diffusion of bulk molecules to (and from) the active sites, (ii) the higher dispersion of these inorganic clusters, which play a crucial role in catalysis and (iii) the robustness of the hybrid materials gained by the replication process.

These materials exhibit higher activity in Michael addition, Henry condensation and for jasminaldehyde synthesis. The higher catalytic activity of these hybrid materials is the more remarkable result given that any pair or these materials (chitosan or inorganic oxide) do not give individually satisfactory results in catalysis. *The increasing catalytic activity was rationalized by the coexistence in close proximity of the basic sites (NH_2 from biopolymer) and the acid sites (metallic center) through their cooperative effect.* The simple preparative procedure, easy recovery and reusable catalytic systems are expected to contribute to the development of benign chemical processes and products. Current efforts aim at taking advantages of these new catalysts to perform complex reactions and to get more insight into the precise mode of action of such acid–base cooperative systems.

Acknowledgments

The authors are grateful to Dr. Claude Guimon (XPS measurements), Thomas Cacciaguerra (X-ray diffraction, SEM and TEM analyses), Geraldine Layrac (TGA and DSC analyses) and Prof. Ron Hibbeln for his technical assistance. The Hassan II Academy of Science and Technology, Morocco and CARNOT foundation (07CARN 00301), France are highly thanked for their financial support.

Appendix A. Supplementary material

Supplementary data associated with this article can be found, in the online version, at doi:10.1016/j.jcat.2010.05.010.

References

[1] 1.G. Kartha, J. Bello, D. Harker, Nature 213 (1967) 862–865.
[2] P. Carter, J.A. Wells, Nature 332 (1988) 564–568.
[3] T. Hoffmann, G.F. Zhong, B. List, D. Shabat, J. Anderson, S. Gramatikova, R.A. Lerner, C.F. Barbas, J. Am. Chem. Soc. 120 (1998) 2768–2779.
[4] E.W. Debler, S. Ito, F.P. Seebeck, A. Heine, D. Hilvert, I.A. Wilson, Proc. Natl. Acad. Sci. USA 102 (2005) 4984–4989.
[5] V.L. Schramm, Curr. Opin. Struct. Biol. 15 (2005) 604–613.
[6] W.M. Atkins, S.G. Sligar, Curr. Opin. Struct. Biol. 1 (1991) 611–616.
[7] J. Kraut, Annu. Rev. Biochem. 46 (1977) 331–358.
[8] S. Saito, H. Yamamoto, Acc. Chem. Res. 37 (2004) 570–579.
[9] A. Peschiulli, Y. Gun'ko, S.J. Connon, J. Org. Chem. 73 (2008) 2454–2457.
[10] Y.-M. Lin, J. Boucau, Z. Li, V. Casarotto, J. Lin, A.N. Nguyen, J. Ehrmantraut, Org. Lett. 9 (2007) 567–570.
[11] A. Chuma, H.W. Horn, W.C. Swope, R.C. Pratt, L. Zhang, G.G. Lohmeijer, C.G. Wade, R.M. Waymouth, J.L. Hedrick, J.E. Rice, J. Am. Chem. Soc. 130 (2008) 6749–6754.
[12] S. Wei, D.A. Yalalov, S.B. Tsogoeva, S. Schmatz, Catal. Today 121 (2007) 151–157.
[13] H. Groger, Chem. Eur. J. 7 (2001) 5246–5251.
[14] M. Boronat, M.J. Climent, A. Corma, S. Iborra, R. Montón, M.J. Sabater, Chem. A: Eur. J. 16 (2010) 1221–1231.
[15] D.W. Stephan, Org. Biomol. Chem. 6 (2008) 1535–1539.
[16] D.W. Stephan, G. Erker, Angew. Chem. Int. Ed. 49 (2010) 46–76.
[17] A. Corma, H. Garcia, Top. Catal 48 (2008) 8–31. 48.
[18] A.R. Vaino, K.D. Janda, J. Comb. Chem. 2 (2000) 579.
[19] A. Corma, Catal. Rev. 46 (2004) 369–417.
[20] J.M. Notenstein, A. Katz, Chem. Eur. J. 12 (2006) 3954–3965.

[21] N. Madhavan, C.W. Jones, M. Weck, Acc. Chem. Res. 41 (2008) 1153–1165.
[22] J. Guzman, S. Carrettin, J.C. Fierro-Gonzalez, Y. Hao, B.C. Gates, A. Corma, Angew. Chem. Int. Ed. 44 (2005) 4778–4781.
[23] A. Abad, P. Concepción, A. Corma, H. García, Angew. Chem. Int. Ed. 44 (2005) 4066–4069.
[24] Y. Tang, S. Miao, B.H. Shanks, X. Zheng, Appl. Catal. A: Gen. 375 (2010) 310–317.
[25] .A. Corma, H. García, A. Leyva, A. Primo, Appl. Catal. A: Gen. 257 (2004) 77–83.
[26] A. Corma, H. García, A. Leyva, Appl. Catal. A: Gen. 236 (2002) 179–185.
[27] A. Corma, H. García, A. Leyva, A. Primo, Appl. Catal. A: Gen. 247 (2003) 41–49.
[28] A. Corma, T. Ródenas, M.J. Sabater, Chem. Eur. J. 16 (2010) 254–260.
[29] A. Corma, C. González-Arellano, M. Iglesias, M.T. Navarro, F. Sánchez, Chem. Commun. (2008) 6218–6220.
[30] B. Voit, Angew. Chem. Int. Ed. 45 (2006) 4238–4240.
[31] B. Helms, S.J. Guillaudeu, Y. Xie, M. McMurdo, C.J. Hawker, J.M.J. Frechet, Angew. Chem. Int. Ed. 44 (2005) 6384–6387.
[32] K. Motokura, D. Nishimura, K. Mori, K. Mizugaki, K. Ebitani, K. Kaneda, J. Am. Chem. Soc. 126 (2004) 5662.
[33] F. Gelman, J. Blum, D. Avnir, Angew. Chem. Int. Ed. 40 (2001) 3647–3649.
[34] E.L. Margelefsky, R.K. Zeidan, M.E. Davis, Chem. Soc. Rev. 37 (2008) 1118–1126.
[35] M. Tada, K. Motokura, Y. Iwasawa, Top. Catal. 48 (2008) 32–40.
[36] M.J. Climent, A. Corma, H. Garcia, R. Guil-Lopez, S. Iborra, V. Fornés, J. Catal. 197 (2001) 385–393.
[37] M.J. Climent, A. Corma, S. Iborra, A. Velty, J. Mol. Catal. A: Chem. 182–183 (2002) 327–342.
[38] M.J. Climent, A. Corma, V. Fornés, R. Guil-Lopez, S. Iborra, Adv. Synth. Catal. 344 (2002) 1090–1096.
[39] K.K. Sharma, T. Asefa, Angew. Chem. Int. Ed. 46 (2007) 2879–2882.
[40] M.W. McKittrick, C.W. Jones, J. Am. Chem. Soc. 126 (2004) 3052–3053.
[41] J.C. Hicks, R. Dabestani, A.C. Buchanan, C.W. Jones, Chem. Mater. 18 (2006) 5022–5032.
[42] E.L. Margelefsky, A. Bendjeriou, R.K. Zeidan, V. Dufaud, M.E. Davis, J. Am. Chem. Soc. 130 (2008) 13442–13449.
[43] J. Alauzun, A. Mehdi, C. Reye, R.J.P. Corriu, J. Am. Chem. Soc. 128 (2006) 8718–8719.
[44] R. Mouawia, A. Mehdi, C. Reye, R.J.P. Corriu, J. Mater. Chem. 18 (2008) 4193–4203.
[45] K. Motokura, M. Tada, Y. Iwasawa, J. Am. Chem. Soc. 131 (2009) 7944.
[46] A. Puglisi, R. Annunziata, M. Nenaglia, F. Cozzi, A. Gervasini, V. Bertacche, M.C. Sala, Adv. Synth. Catal. 351 (2009) 219–229.
[47] K. Motokura, M. Tomita, M. Tada, Y. Iwasawa, Chem. Eur. J. 14 (2008) 4017–4027.
[48] S. Huh, H.T. Chen, J.Z. Wiench, M. Pruski, V. S.-Y. Lin, Angew. Chem. Int. Ed. 44 (2005) 1826–1830.
[49] J.D. Bass, A. Solovyov, A.J. Pascall, A. Katz, J. Am. Chem. Soc. 128 (2006) 3737–3747.
[50] S. Shylesh, A. Wagener, A. Seifert, S. Ernst, W.R. Thiel, Angew. Chem. Int. Ed. 48 (2009) 1–5.
[51] N. Katir, A. El Kadib, M. Dahrouch, A. Castel, N. Gatica, Z. Benmaarouf, P. Riviere, Biomacromolecules 10 (2009) 850–857.
[52] A. El Kadib, N. Katir, N. Marcotte, K. Molvinger, A. Castel, P. Riviere, D. Brunel, J. Mater. Chem 19 (2009) 6004–6014.
[53] N. Katir, A. El Kadib, A. Castel, P. Riviere, Z. Benmaarouf, Appl. Organometal. Chem. 22 (2008) 402–406.
[54] R. Valentin, K. Molvinger, F. Quignard, D. Brunel, New J. Chem. 27 (2003) 1690–1692.
[55] K. Molvinger, F. Quignard, D. Brunel, M. Boissiere, J.M. Devoisselle, Chem. Mater. 16 (2004) 3367–3372.
[56] A. El Kadib, K. Molvinger, C. Guimon, F. Quignard, D. Brunel, Chem. Mater. 20 (2008) 2198–220458.
[57] A. El Kadib, K. Molvinger, M. Bousmina, D. Brunel, Org. Lett. 12 (2010) 948–951.
[58] A. El Kadib, K. Molvinger, M. Bousmina, D. Brunel, submitted for publication.
[59] K. Kojima, M. Yoshikuni, T.J. Suzuki, Appl. Polym. Sci. 24 (1979) 1587–1593.
[60] B. Krajewska, Enzyme Micrb. Technol. 35 (2004) 126–139.
[61] J.J.E. Hardy, S. Hubert, D.J. Macquarrie, A.J. Wilson, Green Chem. 6 (2004) 53–56.
[62] E. Guibal, Prog. Polym. Sci. 30 (2005) 71–109.
[63] D.J. Macquarrie, J.J.E. Hardy, Ind. Eng. Chem. Res. 44 (2005) 8499–8520.
[64] M. Rinaudo, Prog. Polym. Sci. 31 (2006) 603–632.
[65] A. Corma, P. Concepción, I. Domínguez, V. Fornes, M.J. Sabater, J. Catal. 251 (2007) 39–47.
[66] V.K. Mourya, N.N. Inamdar, React. Funct. Polym. 68 (2008) 1013–1051.
[67] T.C.O. Mac Leod, V. Palaretti, V.P. Barros, A.L. Faria, T.A. Silva, M.D. Assis, Appl. Catal. A: Gen. 361 (2009) 152–159.
[68] D. Wei, Y. Ye, X. Jia, C. Yuan, W. Qian, Carbohydr. Res. 345 (2010) 74–81.
[69] A. Murugadoss, A. Chattopadhyay, Nanotechnology 192 (2008) 015603.
[70] C. Guarise, F. Manea, G. Zaupa, L. Pasquato, L.J. Prins, P. Scrimin, J. Pept. Sci. 14 (2008) 174–183.
[71] V. Chechik, Annu. Rep. Prog. Chem., Sect. B 104 (2008) 331–348.
[72] S.E.S. Leonhardt, A. Stolle, B. Ondruschka, G. Cravotto, C.D. Leo, K.D. Jandt, T.F. Keller, Appl. Catal. A: Gen. 379 (2010) 30–37.
[73] R. Moucel, K. Perrigaud, J.-M. Goupil, P.-J. Madec, S. Marinel, E. Guibal, A.-C. Gaumont, I. Dez, Adv. Synth. Catal. 352 (2010) 433–439.
[74] H. Fric, U. Schubert, New J. Chem. 29 (2005) 232–236.
[75] S.S. Kisler, J. Phys. Chem. 36 (1932) 52–64.
[76] G.A. Nicholaon, S.J. Teichner, Bull. Soc. Chim. Fr. (1968) 900–1906.
[77] N. Hüsing, F. Schwertfeger, W. Tappert, U. Schubert, J. Non-Cryst. Solids 186 (1995) 37–43.
[78] B. Himmel, H. Bürger, Th. Gerber, A. Olbertz, J. Non-Cryst. Solids 185 (1995) 56–66.
[79] D.W. Hua, J. Anderson, J. Di Gregorio, D.M. Smith, G. Beaucage, J. Non-Cryst. Solids 186 (1995) 142–148.
[80] D.C.M. Dutoit, M. Schneider, A. Baiker, J. Catal. 153 (1995) 165–176.
[81] Y. Mizushima, M. Hori, J. Non-Cryst. Solids 167 (1994) 1–8.
[82] G.S. Grader, Y. Rifkin, Y. Cohen, S. Keysar, Sol–Gel Sci. Technol. 8 (1997) 825–829.
[83] A.C. Pierre, E. Elaloui, G.M. Pajonk, Langmuir 14 (1998) 66–73.
[84] C.J. Brinker, G.W. Scherer, Sol–Gel Science: The Physics and Chemistry of Sol–Gel Processing, Academic Press, San Diego, 1990.
[85] L. Marchese, E. Gianotti, V. Dellarocca, T. Maschmeyer, F. Rey, S. Coluccia, J.M. Thomas, Phys. Chem. Chem. Phys. 1 (1999) 585–592.
[86] Y. Hasegawa, A. Ayame, Catal. Today 71 (2001) 177–187.
[87] E. Gianotti, A. Frache, S. Coluccia, J.M. Thomas, T. Maschmeyer, L. Marchese, J. Mol. Catal. A: Chem. 204–205 (2003) 483–489.
[88] C.D. Wagner, W.M. Riggs, L.E. Davis, J.F. Moulder, G.E. Muilenberg, Handbook of X-ray Photoelectron Spectroscopy, Perkin-Elmer Corp., Eden Prairie, MN, 1979. p 68.
[89] B.W. Glasspoole, J.D. Webb, C.M. Crudden, J. Catal. 265 (2009) 148–154.
[90] S. Jun, J.M. Kim, R. Ryoo, Y.S. Ahn, M.H. Han, Micro. Meso. Mater. 41 (2000) 119–127.
[91] R. Mokaza, J. Phys. Chem. B 103 (1999) 10204–10208.
[92] M. Etienne, A. Walcarius, Talanta 59 (2003) 1173–1188.
[93] R.K. Iller, The Chemistry of Silicon, Wiley, New York, 1979.
[94] M. Etienne, S. Goubert-Renaudin, Y. Rousselin, C. Marichal, F. Denat, B. Lebeau, A. Walcarius, Langmuir 25 (2009) 3137–3145.
[95] L. Jelinek, E. Kovats, Langmuir 10 (1994) 4225.
[96] D. Brunel, A. Cauvel, F. Di Renzo, F. Fajula, B. Fubini, B. Onida, E. Garonne, New J. Chem. 24 (2000) 807.
[97] N. Tanchoux, P. Trens, D. Maldonado, F. Di Renzo, F. Fajula, Colloids Surfaces A: Physiocochem. Eng. Aspects 246 (2004) 1–8.
[98] M. Boronat, A. Corma, M. Renz, P.M. Viruela, Chem. Eur. J. 12 (2006) 7067–7077.
[99] K. Ma, J. You, Chem. Eur. J. 13 (2007) 1863–1871.
[100] C. Palomo, M. Oiarbide, A. Laso, Angew. Chem. Int. Ed. 44 (2005) 3881–3884.
[101] T. Risgaard, K.V. Gothelf, K.A. Jorgensen, Org. Biomol. Chem. 1 (2003) 153–156.
[102] T. Ooi, K. Doda, K. Maruoka, J. Am. Chem. Soc. 125 (2003) 2054–2055.
[103] A. Anan, W. Quellette, K.K. Sharma, T. Asefa, Catal. Lett. 126 (2008) 142–148.
[104] D. Brunel, A.C. Blanc, E. Garrone, B. Onida, M. Rocchia, J.B. Nagy, D.J. Macquarrie, Stud. Surf. Sci. Catal. 142 (2002) 1395–1402.
[105] D. Brunel, Micro. Meso. Mater. 27 (1999) 329–344.
[106] R.K. Zeidan, M.E. Davis, J. Catal. 247 (2007) 379–382.
[107] M.J. Climent, A. Corma, R. Guil-Lopez, S. Iborra, J. Primo, J. Catal. 175 (1998) 70.
[108] S.K. Sharma, H.A. Patel, R. Jasra, J. Mol. Catal. A.: Chem. 280 (2008) 61.
[109] F. Gandara, M.E. Medina, N. Snejko, B. Gomez-Lor, M. Iglesias, E. Gutierrez-Puebla, M. Angeles Monge, Inorg. Chem. 47 (2008) 6791–6795.